LES and RANS simulation of onshore Bessaker wind farm: analysing terrain and wake effects on wind farm performance

2015 J. Phys.: Conf. Ser. 625 012032

(http://iopscience.iop.org/1742-6596/625/1/012032)

Journal of Physics: Conference Series **625** (2015) 012032 doi:10.1088/1742-6596/625/1/012032

LES and RANS simulation of onshore Bessaker wind farm: analysing terrain and wake effects on wind farm performance

Mandar Tabib[1], Adil Rasheed[1] and Trond Kvamsdal[1,2]

[1]Applied Mathematics, SINTEF ICT, Strindveien 4, 7035, Trondheim, Norway
[2] Mathematical Sciences, NTNU, Alfred Getz vei 1, 7491, Trondheim, Norway

E-mail: mandar.tabib@sintef.no, adil.rasheed@sintef.no, trond.kvamsdal@sintef.no

Abstract. This work compares the predictive performance of RANS and LES solver in capturing the effect of terrain and wakes on the performance of the Bessaker wind farm. This 25 turbine wind farm is located in a highly complex terrain and is exposed to predominantly high westerly and south easterly winds. A one-equation sub-grid scale LES turbulence model has been used to help capture the wake dynamics: particularly the effects of wake meandering and wake-turbine interactions. A comparison between RANS and LES models highlights the influence of turbulence model on wake decay and its subsequent effect on prediction of power production. The LES model predicts delayed decay of the wake and more pronounced wake interference leading to a lower power production in wind farm than the RANS case. The RANS model overpredicts turbulence, which cause faster turbulent momentum diffusivity and faster wake recovery. This study has given some insights regarding the power production at Bessaker wind farm for neutral conditions and westerly flow.

1. Introduction

Accurate simulation of turbulent conditions (like, terrain induced turbulence and wakes interference effects) can help in strategizing a wind farm operation and to reduce its cost of energy. The potential of wind energy is immense provided the cost of wind-energy (COE) is competitive. Significant improvements in turbine technology and operating strategies have helped to reduce the COE in recent decades. Research devoted towards accurate estimate of wind resource can reduce the COE by enabling optimized power production. Wind resource within a particular farm site is influenced by surrounding terrain conditions, atmospheric stratification and wake effects (wherein upstream turbine generated wake influences downstream turbines) [1]-[4]. A model that resolves the large scale dynamics (like LES) can help to more accurately capture the turbulence than the RANS model (which models all the turbulent scales rather than resolving it). However, most of the numerical wind models used to predict wind conditions/power production over simplify the actual physics for the sake of faster computational time, in at least one of these three ways (a) by using less advanced turbulence models, like RANS model in place of the LES model, (b) by not accounting for a complex terrain and over simplifying its effect by using a roughness factor and a flat terrain, (c) by assuming only neutral atmospheric conditions and ignoring stratified conditions and accompanying buoyancy effects. Simulations involving these physics needs large computational resources, while with simplified assumptions

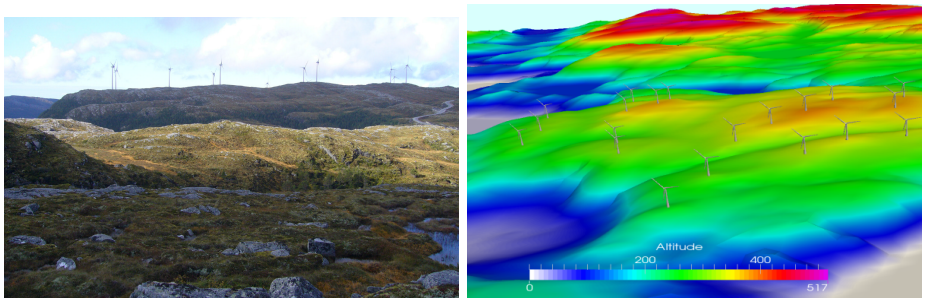

(a) Bessaker wind farm (b) Digital model

Figure 1. Bessaker wind farm

faster results are obtained for enabling engineering solutions which makes them more popular. However, such simplifications are bound to cause a loss of information and accuracy. Many notable contributions have been made to study the gain in accuracy and information using LES turbulence models ([2],[5]-[14]), in case of both the single-turbine and multi-turbine set-ups. These works have helped to highlight the importance of LES, but they have mostly been applied to very simplistic terrain or flatter terrains or off-shore conditions. In this work, we compare the effect of using an LES turbulence model vis-a-vis RANS turbulence model for an industrial scale wind farm located on a highly complex terrain. This model has been applied on a realistic industrial wind farm called Bessaker Wind Farm, operated by Trønder-Energi. The technical aspects about the Bessaker Wind Farm is given in the next section, followed by details of this model, solution methodology, results and discussion and conclusions.

2. Terrain and Bessaker wind farm details

Figure 1 shows the Bessaker wind farm, which is located on a complex terrain in mid-Norway region. This farm is operated by one of the largest energy providers in Norway: Trønder Energy AS. The terrain has an altitude difference of about $500m$, starting from sea level to the highest peak. This terrain houses 25 turbines of Enercon E70 turbine make. The lowest turbine base is located at $240m$ above sea level and the highest turbine is located at about $385m$ above sea level. The rest of the turbines are within this altitude range. All turbines have a rated power of $2.3MW$ with rotor diameter of $71m$ and a hub height of $64m$. The cut-off speed is about $28m/s$ wind. Generally, most dominant wind directions recorded at this site at $35m$ above the ground is westerly and south easterly and the average wind speed is recorded in the range of $10-15m/s$ implying that the turbines are rarely idle. However, a closer look at the power production of individual turbines reveals that a few turbines are almost always underperforming and overall power production is low. Computational Fluid Dynamics simulations were used to understand why this could be occurring. Our previous RANS based studies suggested that this drop in power production at wind farm could be owing to flow channeling and delayed wake decay [15]-[16] due to thermal stratification. This current work is conducted for neutral conditions and helps to understand the effect of turbulence modelling on wakes and power production in wind farm.

3. CFD Model and Equations solved

3.1. Governing Equations

A transient 3D CFD model incorporating the actuator line model is developed. The model computes the flow field (velocity, pressure, temperature) and the turbulence field arising out of shear induced turbulence, buoyancy induced turbulence and turbine induced wake effects in

the wind farm. The turbulence is modeled using two different turbulence models: One-equation sub-grid scale turbulent kinetic energy LES model and the RANS k-ϵ model. The equations for LES are derived by applying filtering operator to the NavierStokes equations, while equations for RANS are derived by applying the Reynolds averaging to the Navier-Stokes equations. The equation set for both cases can be represented by Equations 1-**??**, where velocity $\mathbf{u}$ represents the filtered (or resolved) velocity in-case of LES and the ensemble averaged velocity in case of RANS. Thus, the three equations below represents a filtered (or averaged) mass continuity equation (Equation 1), filtered (or averaged) and momentum transport equation (Equation 2).

$$\nabla \cdot (\rho \mathbf{u}) = 0 \tag{1}$$

where ρ is the density.

$$\frac{D\mathbf{u}}{Dt} = -\nabla \left(\frac{p}{\rho}\right) + \frac{1}{\rho}\nabla \cdot \mathbf{R} + \mathbf{f} \tag{2}$$

where, p is pressure, t is time, $\mathbf{f}$ refers to external forces arising from actuator line model, $R_{ij} = \nu_T \left(\frac{\partial u_i}{\partial x_j} + \frac{\partial u_j}{\partial x_i}\right) - \frac{2}{3}k\delta_{ij}$ arises owing to averaging procedure and is referred to turbulent stresses. The computation of eddy viscosity needed for the closure of above equation set is dependent upon the turbulence model (as described below). When $k - \epsilon$ model is used, the turbulent eddy viscosity is formulated in terms of turbulent kinetic energy (k) and eddy dissipation rate (ϵ). These two are obtained by solving their transport equation as in Equation 4 and 5.

$$\mu_t = C_\mu \frac{k^2}{\epsilon} \tag{3}$$

where C_μ is a constant.

$$\frac{DK}{Dt} = \nabla \cdot \left(\frac{\nu_T}{\sigma_k}\nabla K\right) + P_k - \epsilon \tag{4}$$

$$\frac{D\epsilon}{Dt} = \nabla \cdot \left(\frac{\nu_T}{\sigma_e}\nabla \epsilon\right) + (C_1 P_k)\frac{\epsilon}{k} - C_2\frac{\epsilon^2}{k} \tag{5}$$

where ν_T is turbulent diffusivity, σ_e and σ_e are turbulent prandtl numbers, P_k is production of turbulent kinetic energy due to shear. The production due to buoyancy term is neglected here for neutral flows.

$$P_k = \nu_T \left(\frac{\partial u_i}{\partial x_j} + \frac{\partial u_j}{\partial x_i}\right)\frac{\partial u_i}{\partial x_j} \tag{6}$$

When LES model is used, the turbulent eddy viscosity is formulated as follows:

$$\mu_t = \rho(C_k \Delta) k_{sgs}^{1/2} \tag{7}$$

where C_k is a constant and k_{sgs} is obtained by solving a transport equation for sub-grid scale turbulent kinetic energy. The value of C_k used in this study is 0.094.

3.2. Actuator Line Model

The turbines are modeled using actuator line model (ALM) approach, which was first developed by Sørensen and Shen [17] . The actuator line model (Equations 8, 9 and 10) uses the velocity field input from the CFD model and outputs body force, which are used as the sink term in the momentum equation. The ALM approach resolves each blade of the turbine as a rotating line (made of N actuator segments), over which the forces are computed. The force at each segment comprises of lift force and drag forces (Equations 8, 9), which are computed from the local relative velocity (V_{rel}) , local twist angle, blade chord (c), local actuator width (w) and local

angle of attack (α) at a given actuator segment. The local angle of attack is computed from the tangential and normal component of relative velocity at the segment. The lift coefficient (C_l) and drag coefficient (C_d) at each segment (in Equations 8, 9 and 10) are a function of local angle of attack, and this dependency is provided as an input (blade airfoil data) to the ALM model. The force at an actuator segment i (f_i) is a point force and it is translated on to the fluid domain as a volumetric body force (F_i) using Gaussian projection (Equation 10). The regularization parameter (ε) in Equation 10 represents the width of the Gaussian and determines the concentration of the force. Larger the parameter, more smoothed out the force is on the flow field. The negative sign in Equation 10 accounts for the fact that the force exerted by turbine on the flow field is equal and opposite to the force experienced by it due to the flow. At the location (x, y, z) of the fluid domain, the overall body force is summation of force over all N actuator segments of the turbine, where (x_j, y_j, z_j) is the location of the j^{th} segment and r_j is the distance between segment j and the fluid domain location. In the present work, the aerodynamic data for Enercon E70 turbine blades was not available. So, we modified the aerodynamic data for NREL 5MW Reference blade such that a power-curve similar to an Enercon E70 blade is obtained.

$$L = \frac{1}{2} C_l(\alpha) \rho V_{rel}^2 cw \tag{8}$$

$$D = \frac{1}{2} C_d(\alpha) \rho V_{rel}^2 cw \tag{9}$$

$$F_i^T(x, y, z) = -\sum_{j=1}^{N} f_i^T(x_j, y_j, z_j, t) \frac{1}{\varepsilon^3 \pi^{3/2}} exp\left[-\frac{r_j^2}{\varepsilon}\right] \tag{10}$$

4. Simulation methodology : Solver details and set-up parameters

4.1. Solver details

The solver has been created in OpenFOAM-2.3.0 (OF). To ensure continuity, an elliptic equation for the modified pressure is created by combining continuity equation with divergence of momentum equation. This elliptic equation along with the momentum equation, energy equation and turbulence equation are solved in a segregated manner using the PISO-SIMPLE algorithm (PIMPLE algorithm). The PIMPLE algorithm ensures use of a higher time step for transient simulations. The OF uses a finite volume discretization technique, wherein all the equations are integrated over control volumes (CV) using Green Gauss divergence theorem. The gauss divergence theorem converts the volume integral of divergence of a variable into a surface integral of the variable over faces comprising the CV. Thus, the divergence term defining the convection terms can simply be computed using the face values of variables in the CV. The face values of variables are obtained from their neighboring cell centered values by using convective scheme. In this work, all the equations (except k and turbulence equations) use second order linear discretization scheme, while the turbulent equations use upwind convection schemes. Similarly, the diffusion term involving Laplacian operator (the divergence of the gradient) is simplified to computing the gradient of the variable at the face. The gradient term can be split into contribution from the orthogonal part and the non-orthogonal parts, and both these contributions have been accounted for. The mesh details, CFD domain set up, boundary and initial conditions are defined below.

4.2. CFD set up

The Bessaker wind farm CFD set up involves a domain size of $6.98km \times 4.7km \times 1.3km$ (Figure 2). This domain size ensures that the entire wind/farm area is considered and the location of domain boundary will not affect the flow profile within wind farm. A westerly wind flow is

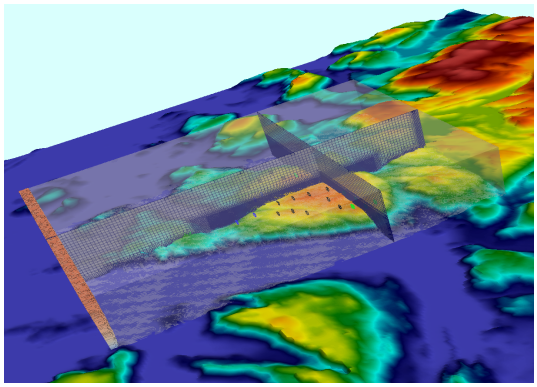

Figure 2. CFD domain and internal mesh enclosing the terrain. Westerly wind flows from inlet at the left and the outlet on right. Top and side walls are slip boundary.

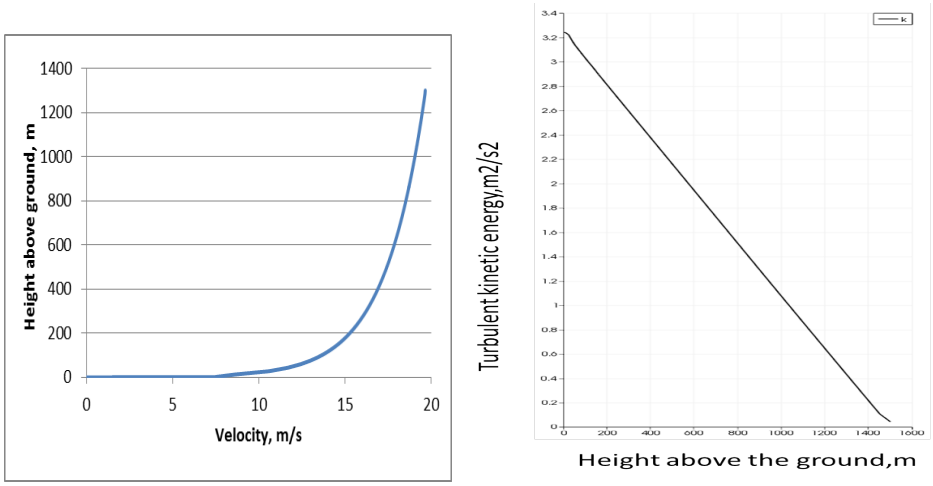

(a) Inlet Velocity (b) Inlet turbulent kinetic energy

Figure 3. Inlet boundary profiles

considered for this simulation as this is one of the dominant wind directions at the site. The terrain geometry is included in the domain as an stereo lithography file (STL) and the domain and mesh is built using it. The mesh size for this domain is about 13 million cells. The grid is finer in the wind farm region and near the terrain, where the velocity gradient is high and effect of wake has to be captured. The finest grid size is $6m$ in the wind farm location. This ensures that there are at least 10 numerical finite volume cells within the turbine area, as the rotor blade is of $60m$ diameter. The time step used for simulation is more stringent than normal CFL criteria of 1. This time step was selected based on the tip speed and grid cell size in the actuator line model domain. The time step was such that the blade (rotating line) does not move more than one grid cell within a time step. To achieve this, a time step of $0.015s$ was used which gave a CFL of 0.12. An Euler discretization scheme is chosen for temporal discretization. The solver was run on 216 parallel processors. The simulation has been carried out for two cases: (a) RANS neutral atmospheric condition and (b) LES neutral atmospheric condition. Figure 3 shows the inlet conditions specifed as a function of vertical distance from ground : velocity profile is used in both LES and RANS case and the inlet turbulent kinetic energy profile is used only for RANS study. No potential temperature equation is required to be solved for the neutral

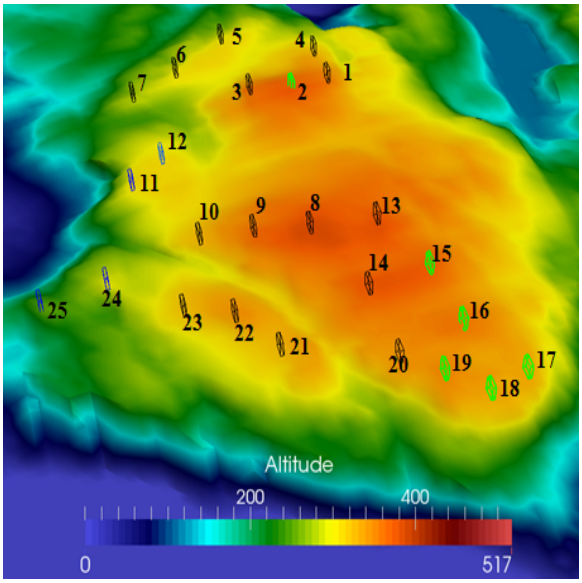

Figure 4. Location and performance of 25 Turbines. Green coloured turbines producing highest power, blue coloured turbine producing lowest power and rest black coloured are in between

boundary condition. The side and top boundary conditions of the domain are slip walls. The outlet has fixed pressure boundary conditions. The bottom terrain geometry is no-slip boundary condition. A continuouse wall function for rough wall as suggested by Spalding[18] has been used to simulate the near wall profiles. Figure 4 shows the location of the 25 turbines on the terrain. The effect of turbines is accounted using the actuator line method as explained in section 3. For the actuator line method, about 40 actuator segments (i.e parameter N in equation 10) in were used in the simulation. The regularization parameter (ε in equation 10) in ALM was chosen to be about two times the cube root of grid volume size in that region. This was selected so as to ensure that the force is not overly concentrated to cause numerical oscillations/solver instability, and neither does the force becomes too smoothed so as to cause no resistance to the wind flowing through the turbine. The LES runs were initialized from the RANS runs. The LES results were run for 6500 s of simulation time (which corresponds to approximately 15 times flow passage in the domain at wind free stream velocity,nearly 18m/s) and averaging was done for last 3000 s. The simulation took around 3 weeks of computational time when run parallely on 216 processors (each processor having 2.6 GHz processing speed). The next section discusses the results obtained.

5. Results and discussions

5.1. Prediction of power produced by RANS and LES

For neutral atmospheric conditions and westerly wind direction, the overall power output predicted in the wind farm by RANS Simulation ($30 - 31MW$) is around $8 - 10\%$ more than that predicted by LES simulation (around $27.528MW$). Most of the turbines produce higher power with RANS simulation than for the LES simulation. The reasons for this is the way turbine induced wake effects and terrain induced effects are captured by the two turbulence models (explained in sections below).

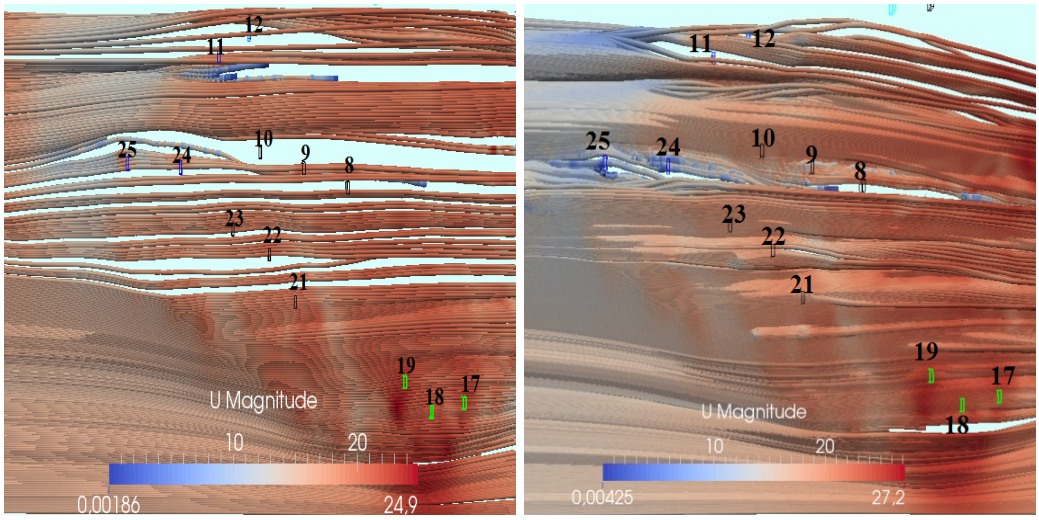

(a) RANS streamline (b) LES instantaneous streamline

Figure 5. Turbine performance : green coloured turbines (number 15-19) are exposed to higher velocity wind and perform well while blue coloured turbines (number : 25,24,11,12 in streamline) perform the worst owing to lower wind-velocity.

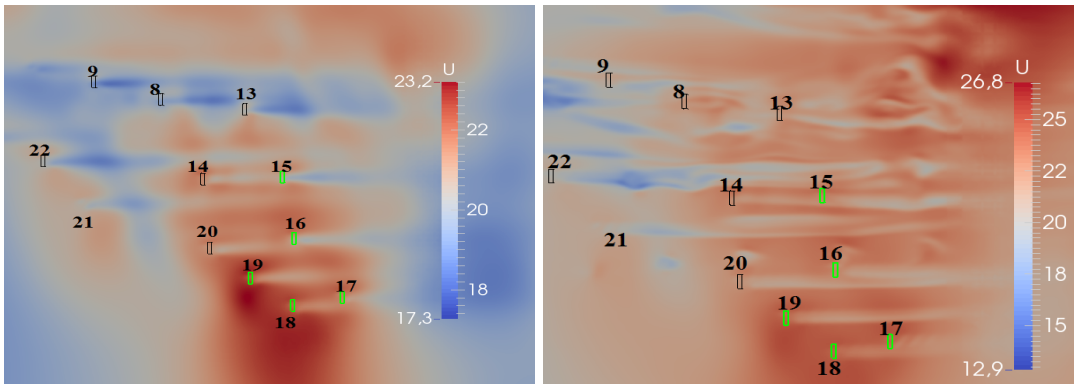

(a) RANS velocity at a given instant (b) LES instantaneous velocity

Figure 6. Comparision of RANS and LES velocity at a instant and relation to turbine performance

5.2. Terrain effects and wake effects captured by the two models

The atmospheric wind when exposed to any terrain related obstructions undergoes a change in its flow pattern. This involves wind speed-up over the hill, boundary layer separations, channeling, mountain waves, etc. Turbulence generated by rough terrain plays an important role in diffusing momentum and it affects the flow pattern. Figure 5-6 compares results at a given instant for streamline and velocity, while figures 7-9 compares the mean-fields of velocity,vorticity and turbulent knietic energy. In all the figures, the turbine numbers are marked to enable easy comprehension. The figures 7-9 are plotted by merging two planes on a common color-map : the plane involving turbine 8,9 and 13 at top is located at a higher altitude of 435 m (to capture the wakes at their hub height) and the plane at bottom involving rest of turbines is located at altitude of 405 m. Figure 5 shows that for both the turbulence models, the turbines shown in

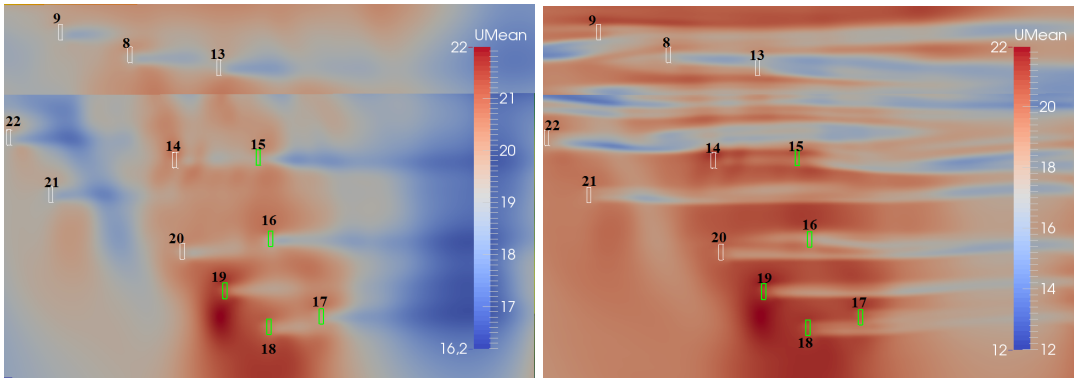

(a) RANS predicted mean velocity (b) LES predicted mean velocity

Figure 7. Mean velocity contours

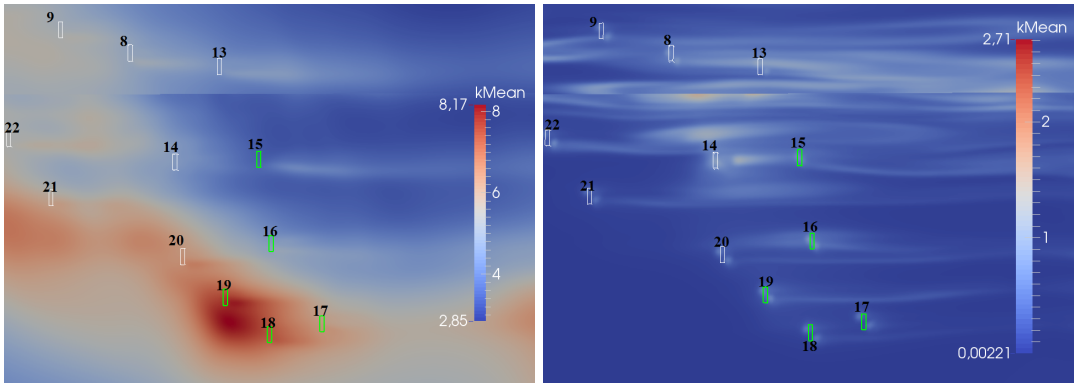

(a) RANS (b) LES

Figure 8. Mean turbulent kinetic energy contours

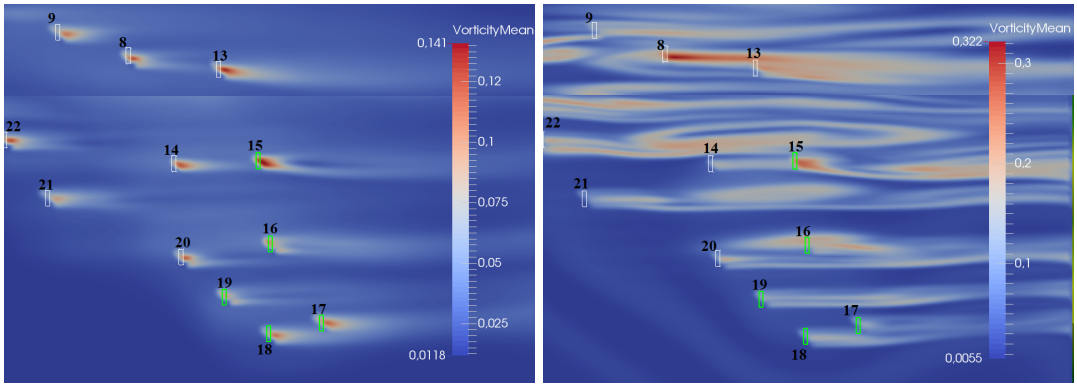

(a) RANS (b) LES

Figure 9. Mean vorticity contours

green color in Figure 5 (Turbine number 15, 16, 17, 18, 19) are producing higher power output, while the turbines shown in blue color (Turbine number 11, 12, 24, 25) are producing the least power output. The reason for this behavior can be attributed to the wind flow experienced by these turbines. The instantaneous streamlines obtained from LES (in Figure 5(b)) shows higher velocity wind region (wind speed above $20m/s$, up-to $27m/s$) at location of green colored turbines. These turbines are located at higher altitude and experience good wind speeds owing to speed-up over altitude. While, the turbines in blue are at lower altitude and experience comparatively lower wind speed between $5 - 10m/s$ and hence, provides lower power output. Similar trends were observed by streamlines from RANS model [16] as shown in Figure 5(a) , except that the obtained velocity range was different than LES. RANS revealed wind-speeds of about $15 - 22m/s$ in the high altitude regions where the better performing green colored turbines lie, and wind speeds of $5 - 15m/s$ at lower altitude regions where low performing blue colored turbines lie. The instantaneous LES velocity contour (Figure 6(b)) also shows a wider velocity range (difference between the minimum and maximum velocity values) than the RANS predicted field (Figure 6(a)) at a given instant. Figure 7 compares the time-averaged velocity predicted by LES and RANS. The comparision shows that LES predicts a more pronounced wake region than RANS and thus more downstream turbines are exposed to wakes with lower velocity. For example, compare the wake behind turbines 8-13, 14-15, 16-20 and 17-21 (in Figure 7-9) for the two cases of RANS and LES. These figures shows that LES predicts higher wake interference effect, which results in a lower prediction of power production as compared to RANS. The differences in prediction of wake effect by the two models could be because of the way the shear induced turbulence (owing to terrain and velocity gradient in atmospheric flow) are captured. RANS models predict higher values of time-averaged turbulent kinetic energy than the LES (as seen in Figure 8) , which causes larger turbulent momentum diffusivity. This results in faster wake decay. The overall effect is that for RANS simulations the turbines are exposed to a wind profile that causes higher overall power production. This is seen in vorticity plots too. Figure 9 compares the time-averaged vorticity plot obtained from LES and RANS. The LES mean vorticity plot reveals that wakes induced by turbine 8 reaches out further till turbine 13, and similar wake interference can be seen in turbine 14-15 and turbine 17-18. In contrast, in the RANS vorticity prediction, the wake vortices seems to decay faster. Also, a higher degree of meandering of wakes is observed in LES case than in RANS. Thus, for the current study involving westerly wind direction, the current inter-turbine distance (around four times the rotor diameter between turbines 14-15) leads to an inefficient windfarm operation perspective. However, in-order to draw a general criteria about optimum inter-turbine spacings, more studies at different wind conditions and inter-turbine spacings needs to be done.

6. Conclusion and future work

A one-equation sub-grid scale turbulent kinetic energy LES model and a RANS turbulence model have been used to observe the wake dynamics and the power production in an industrial multi-turbine wind farm. Both the models incorporate the actual terrain effects along with an actuator line model for understanding wake behaviour. The RANS model predicts a higher power production in wind farm than the LES as it predicts faster decay of the wake. This is owing to higher terrain induced and wake turbulence predicted by RANS model, which cause faster turbulent momentum diffusivity and faster wake recovery. The LES model reveals that for this particular wind farm layout, terrain and wind direction condition, the placement of downstream turbines at an inter-turbine distance of four rotor turbine diameter is not good from wind farm operation perspective owing to wake interference. The RANS shows the wake effects but the turbine-turbine wake interactions is not as pronounced as in LES. To draw a general criteria about optimum turbine spacings, more studies at different wind conditions and inter-turbine spacings needs to be done. Future work may also involve inclusion of stratification

effects in LES model for wake-plume interaction and nesting the meso-scale CFD model with the LES model for better inlet boundary conditions.

Acknowledgments
The authors would like to acknowledge the financial support from the Norwegian Research Council and the industrial partners of the FSI-WT (216465/E20) (http://www.fsi-wt.no) project (Kjeller Vindteknikk, Statoil, Trønder Energi AS and WindSim). We are also thankful to Ingrid Vik and Magne Røen from TrønderEnergie for providing information on the locations of turbines in the Bessaker wind farm and the information on turbines.

References

[1] Churchfield MJ, Lee S, Michalakes J, Moriarty PJ, A numerical study of the effects of atmospheric and wake turbulence on wind turbine dynamics,*Journal of Turbulence* 2012;N14.
[2] Churchfield MJ, Lee S, Moriarty PJ, Martnez LA, Leonardi S, Vijayakumar G, Brasseur JG, A large-eddy simulation of wind-plant aerodynamics, 50th AIAA Aerospace Sciences Meeting Including the New Horizons Forum and Aerospace Exposition, 2012
[3] Keck RE, Maré MDe, Churchfield MJ, Lee S, Larsen G, Madsen HA, On Atmospheric Stability in the Dynamic Wake Meandering Model, *Wind Energy* , 2014;17:1689-1710.
[4] Lee S, Churchfield MJ, Moriarty PJ, Jonkman J, Michalakes J, A Numerical Study of Atmospheric and Wake Turbulence Impacts on Wind Turbine Fatigue Loadings, *Journal of Solar Energy Engineering*, 2013;135(3):31001-10
[5] Calaf M, Meneveau C, Meyers J. (2010). Large eddy simulation study of fully developed wind-turbine array boundary layers. *Physics of Fluids*, 22 (1), art.nr. 015110, 1-16.
[6] Jimenez A, Crespo A, Migoya E, Garcia J. 2008, Large-eddy simulation of spectral coherence in a wind turbine wake, *Environmental Research Letters*, 3(1),
[7] Martnez-Tossas LA, Churchfield MJ and Leonardi S. 2014,Large eddy simulations of the flow past wind turbines: actuator line and disk modeling, *Wind Energy* 2014,
[8] Mehta D, Zuijlen AH, Koren B, Holierhoek JG, Bijl H. 2014 Large Eddy Simulation of wind farm aerodynamics: A review, *Journal of Wind Engineering and Industrial Aerodynamics* 2014, 133, 1-17.
[9] Porté-Agel F, Wu YT, Lu H, Conzemius RJ. 2011. Large-eddy simulation of atmospheric boundary layer flow through wind turbines and wind farms. *Journal of Wind Engineering and Industrial Aerodynamics* 99(4): 154-168.
[10] VerHulst C and Meneveau C. 2014 Large eddy simulation study of the kinetic energy entrainment by energetic turbulent flow structures in large wind farms, *Physics of Fluids* 26, 025113
[11] Basu S, Porté-Agel F. 2006. Large-eddy simulation of stably stratified atmospheric boundary layer turbulence: A scale-dependent dynamic modeling approach. *Journal of the Atmospheric Sciences* 63(8): 2074-2091.
[12] Lu H, Porté-Agel F. 2011. Large-eddy simulation of a very large wind farm in a stable atmospheric boundary layer. *Physics of Fluids* 23(6).
[13] Wan F, Porté-Agel F. 2011b. Large-Eddy Simulation of Stably-Stratified Flow Over a Steep Hill. *Boundary-Layer Meteorology* 138(3): 367-384.
[14] Wu YT, Porté-Agel F. 2011. Large-Eddy Simulation of Wind-Turbine Wakes: Evaluation of Turbine Parametrisations. *Boundary-Layer Meteorology* 138(3): 345-366.
[15] Rasheed A, Sørli K, Holdahl R, Kvamsdal T, A Multiscale Approach to Micrositing of Wind Turbines, Energy Procedia 2012;14:1458-1463.
[16] Tabib M, Rasheed A, and Kvamsdal T, Investigation of the impact of wakes and stratification on the performance of an onshore wind farm, Submitted to *Energy Procedia*
[17] Sørensen J, Shen W. 2002. Numerical modelling of Wind Turbine Wakes. *Journal of Fluids Engineering* 124 (2): 393-399.
[18] Spalding D. 1961.A single formula for the law of the wall. *Transactions ofth ASIDE, Series E: Journal of Applied Mechanics* 28,455-458.